Enzymatic oxidation of ellagitannin and a new ellagitannin metabolite from *Camellia japonica* leaves

Takaaki Tsujita, Yosuke Matsuo, Yoshinori Saito, Takashi Tanaka*

Graduate School of Biomedical Sciences, Nagasaki University, 1-14 Bunkyo-Machi, Nagasaki 852-8521, Japan

* Corresponding author. Tel.: +81 95 819 2432;

E-mail address: t-tanaka@nagasaki-u.ac.jp

Polyphenols in the leaves of *Camellia japonica* L. at different stages of growth were analyzed by HPLC. Pedunculagin [2,3;4,6-bis-(*S*)-hexahydroxydiphenoyl-D-glucose] was the major polyphenol in the youngest leaves. The levels of this compound and (+)-catechin decreased as the leaves matured. The level of (-)-epicatechin did not change with leaf maturity. Enzymatic oxidation of pedunculagin was examined to investigate the mechanism of the decrease. Pedunculagin was not directly oxidized by treatment with oxidative enzymes. However, when (+)-catechin was added to the reaction mixture, the pyrogallol rings of the 4,6-hexahydroxydiphenoyl group was oxidatively cleaved to give 2*H*-2-oxo-pyran-6-carboxylic acid. The in vitro oxidation products were not detected in fresh leaves, but two pedunculagin oxidation products conjugated with flavan-3-ol were isolated. A new metabolite, camelliatannin I, was isolated and characterized by spectroscopic and density functional theory calculation of NMR chemical shifts.

Keywords: *Camellia japonica*; ellagitannin; oxidation; catechin; 2*H*-2-oxo-pyran-6-carboxylic acid; camelliatannin

1. Introduction

Tannins are widely distributed in the plant kingdom, and form part of the plant defense system because of their ability to precipitate proteins that cause unpleasant astringent and bitter tastes. These compounds inhibit the digestive enzymes of herbivores, and decrease nutrient absorption.[1] Unlike highly toxic alkaloids and terpenoids, which are targeted to specific biogenic molecules or biological functions, the toxicity of tannins is nonspecific. Therefore, large quantities of tannins are synthesized and accumulate in tannin-containing plants for effective protection against herbivores and microorganisms.[2] However, the relationship between the structures of tannins and their biological functions is unclear. Feeny showed that seasonal changes in the tannins in oak leaves affect feeding behavior of larvae of the winter moth (*Operophtera brumata* L.).[3] In persimmon, proanthocyanidins precipitate when the seeds are ready for germination, and this makes the fruit more enticing to animals to eat and disperse the seeds.[4] Seasonal changes in the tannins in other plant species have also been reported and discussed from various viewpoints, such as chemical ecology and tannin biosynthesis.[5] However, chemical mechanism of the seasonal change of tannins is not fully understood. In our chemical studies on tannin metabolism in plants, we found changes in the tannin composition in the young leaves of *Camellia japonica* L., which is a well-known ornamental flowering tree originating from Japan, Korea, and China.

Young leaves of *C. japonica* collected in April contained the ellagitannin pedunculagin (**1**) and (+)-catechin (**2**), (-)-epicatechin (**3**), and procyanidins as major polyphenols. However, the levels of **1** and **2** in leaves collected in August were negligible. Leaves on a single twig collected in May also showed decreased levels of **1** and **2** with increasing leaf maturity (Figs. 1 and 2). In this paper, we studied enzymatic degradation of **1** assuming that the levels of **1** in the leaves decreased because of oxidative degradation. In addition, the oxidation metabolites of ellagitannins in the leaves were also investigated.

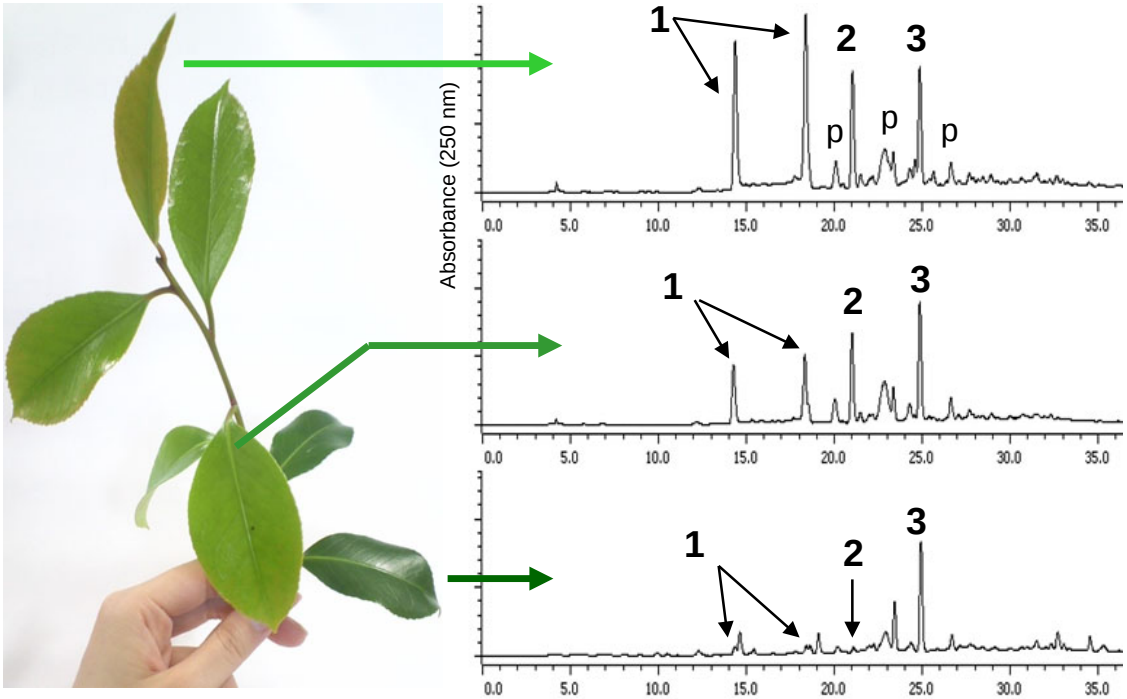

Fig. 1. HPLC profiles of 60% ethanol extracts of the leaves of *C. japonica*.

Compound labels are: **1**, α- and β-anomers of pedunculagin; **2**, catechin; **3**, epicatechin; and p, procyanidins

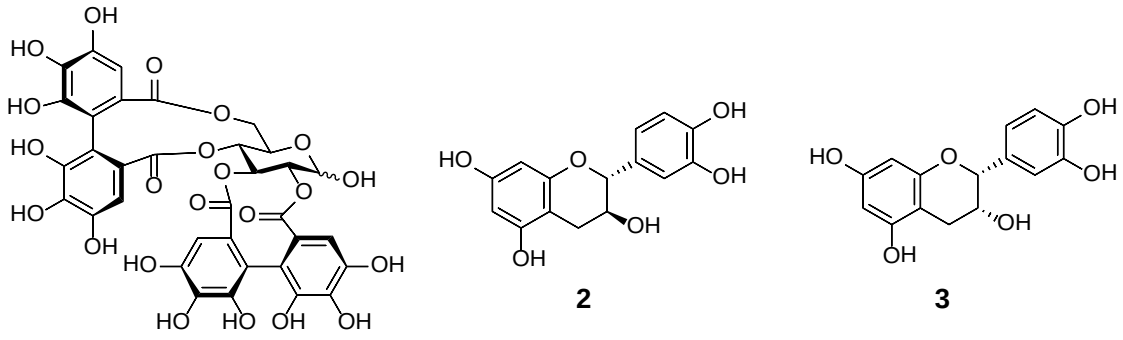

Fig. 2. Structures of major polyphenols found in *C. japonica* leaves.

2. Results and discussion

2.1. Enzymatic oxidation of pedunculagin

Previous studies indicated that *C. japonica* leaves contain dimeric ellagitannins and flavan-3-ol conjugated ellagitannins,[6] which are biogenetically related to **1**. Therefore, conversion of **1** to these metabolites during leaf growth is possible. However, preliminary experiments involving fractionation of extracts of young and mature leaves by Sephadex LH-20 column chromatography, and subsequent HPLC and TLC analyses of the phenolic fractions, did not show an apparent increase of specific ellagitannin

metabolites, including the ellagitannin dimers. Therefore, we assumed that the decrease in **1** was caused by enzymatic oxidation of the pyrogallol rings, because electron rich polyphenols are easily oxidized both chemically and enzymatically as observed in tea leaves during black tea production.[7] We used a homogenate of Japanese pear fruit as a source of polyphenol oxidase by taking account of strong activity of polyphenol oxidase, and the oxidation products of tea catechins are almost the same as that produced during black tea production. Furthermore, Japanese pear fruit homogenate shows practically no background peaks in HPLC analysis and is easily applied to large-scale experiments.[7b,c] In this study, pedunculagin (**1**) was first treated with the Japanese pear fruit homogenate, but this did not oxidize **1** and its levels did not decrease (Fig. 3). Next, (+)-catechin (**2**) was added to the reaction mixture (0.5 molar equivalents), since **2** is also present in *C. japonica* leaves and its level decreases along with that of **1**. Addition of **2** dramatically changed the reaction, and **1** immediately disappeared.

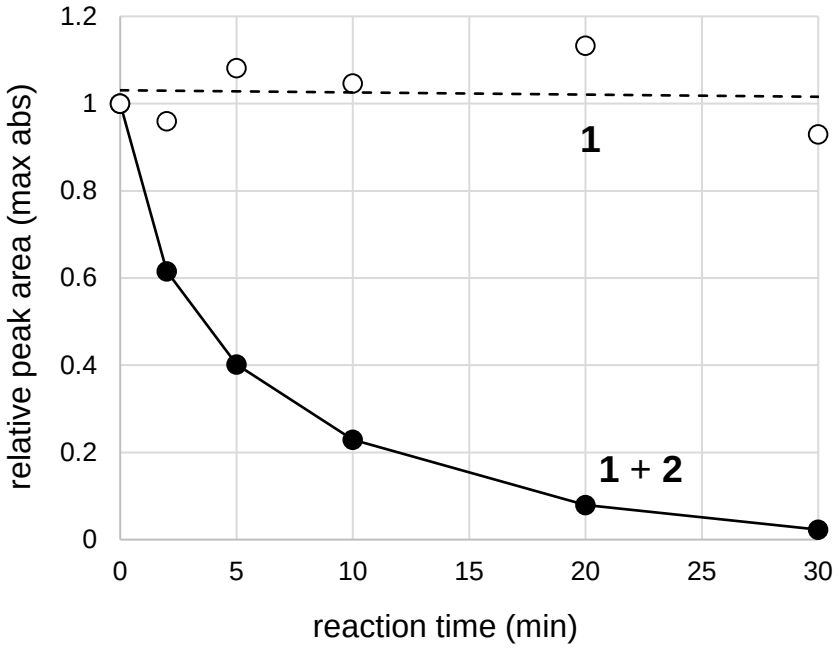

Fig. 3. Decrease in the level of **1** on treatment with polyphenol oxidase

Open circle: **1** + polyphenol oxidase, solid circle: **1** + **2** + polyphenol oxidase

By contrast, when **2** was treated solely with the Japanese pear fruit homogenate, the level of **2** decreased rapidly to give a complex mixture of oxidation products, including dehydrodicatechin-type oligomers.[7c,8] The rate of decrease of **2** was much faster than that in the reaction in the presence of **1**. This could be explained by a coupled oxidation mechanism proposed for catechin oxidation during black tea production,[7c,9] where the enzyme preferentially oxidizes the catechol-B-ring of **2** to *o*-quinone **2a** according to the enzyme specificity. The resulting highly electron deficient *o*-quinone (**2a**) oxidizes the pyrogallol-ring of **1**, which is accompanied by reduction of

2a and reproduction of **2** (Scheme 1).

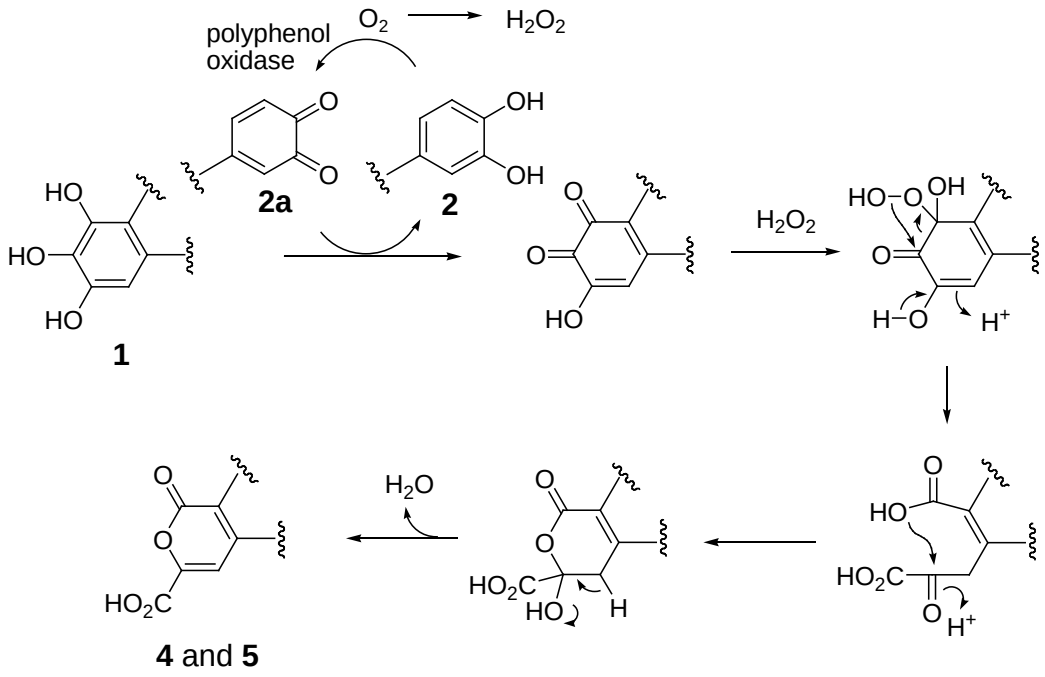

Scheme 1 Plausible oxidation mechanism.

HPLC analysis of the reaction mixture showed many small peaks attributable to the oxidation products, and two products **4** and **5**, which were detected as relatively distinct peaks. These two products were purified by column chromatography using a combination of Sephadex LH-20, polystyrene-gel, and octadecyl silica gel columns. The product **4** showed a peak for $[M+H]^+$ at *m/z* 799, which indicated that its molecular weight was 14 mass units larger than that of **1** (MW 784). The ^1H and ^{13}C NMR data (Table 1) were similar to those of **1**, and showed signals arising from the α- and β-anomers of a tetraacyl glucopyranose together with a hexahydroxydiphenoyl (HHDP)

group. Heteronuclear multiple bond correlation (HMBC) of the ester carbonyl carbons with glucose H-2 and H-3 (Fig. 4) confirmed the HHDP esters were located at the glucose C-2 and C-3 positions. The ^{13}C NMR signals showed the other acyl group attached to the glucose 4 and 6 positions was composed of a pyrogallol ring, two sets of double bonds, and four conjugated carboxyl groups. HMBC of an olefinic proton singlet (H-6: δ_H 7.06, α-anomer, and δ_H 7.02, β-anomer) suggested a 2*H*-2-oxo-pyran-6-carboxylic acid structure (ring C in Fig. 4). Although there were two possible partial structures (**4** and **4a**), **4a** was unlikely because of a ^4J correlation, and this was confirmed by computational calculation (vide infra). HMBC for glucose H-4 with the carboxyl carbon C-7 indicated that this moiety was esterified to the glucose C-4 hydroxy group (Fig. 4).

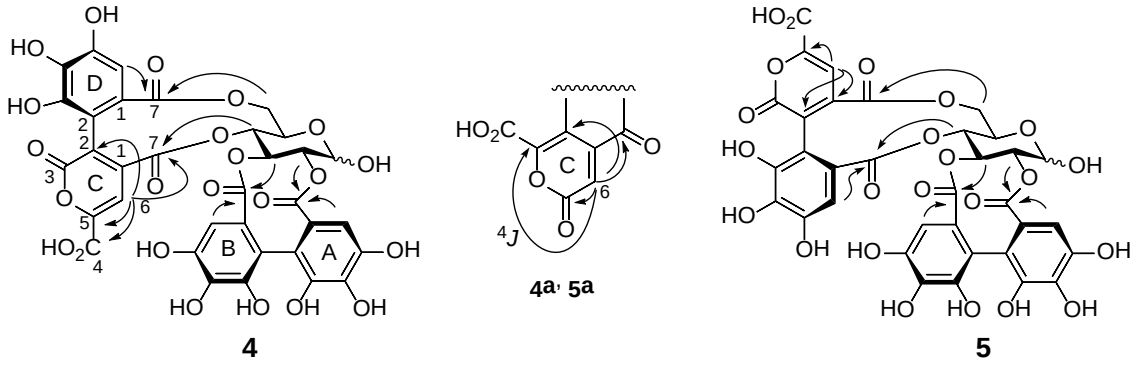

Fig. 4. Selected HMBC results for **4** and **5**.

Table 1 ^{13}C (125 MHz) and ^{1}H (500 MHz) NMR data for **4** and **5** (δ in ppm, *J* in Hz).

	4[a]				**5**[a]			
	α-anomer		β-anomer		α-anomer		β-anomer	
Position	^{13}C	^{1}H	^{13}C	^{1}H	^{13}C	^{1}H	^{13}C	^{1}H
1	91.1	5.41 (d, 3.7)	94.7	5.04 (d, 8.2)	91.0	5.38 (d, 3.7)	94.5	4.97 (d, 8.2)
2	74.9	5.03 (m)	77.5	4.82 (dd, 8.2, 9.3)	75.1	5.02 (dd, 3.7, 9.2)	77.6	4.79 (dd, 8.2, 9.0)
3	75.2	5.44 (t, 9.6)	77.2	5.23 (dd, 9.3, 9.8)	75.1	5.38 (dd, 9.2, 9.8)	76.8	5.19 (dd, 9.0, 10.1)
4	71.2	5.02 (m)	70.8	4.97 (dd, 9.7, 9.8)	70.0	5.09 (t, 9.8)	69.7	5.08 (t, 10.1)
5	66.2	4.64 (ddd, 2.9, 7.0, 10.0)	71.3	4.30 (ddd, 2.3, 6.9, 9.7)	71.2	4.18 (ddd, 1.8, 6.8, 9.8)	66.2	4.55 (ddd, 1.6, 6.8, 10.1)
6a	63.8	5.29 (dd, 7.0, 12.7)	63.6	5.35 (dd, 6.9, 12.9)	65.1	3.96 (dd, 1.8, 12.8)	65.0	4.02 (dd, 1.6, 13.0)
6b		3.86 (dd, 2.9, 12.7)		3.92 (dd, 2.3, 12.9)		4.98 (m)		4.98 (m)
A-1	126.1[b]	-	126.0[b]	-	124.1[c]	-	124.1[c]	-
A-2	114.5	-	114.4	-	114.2	-	114.3	-
A-3	145.0	-	145.0	-	144.0	-	144.0	-
A-4	136.1	-	136.1	-	136.0	-	136.0	-
A-5	144.1	-	144.1	-	144.8	-	144.8	-
A-6	107.4	6.59 (s)	107.4	6.59 (s)	107.2	6.58 (s)	107.2	6.57 (s)
A-7	168.9	-	169.0	-	169.0	-	169.1	-
B-1	125.9[b]	-	126.0[b]	-	125.6[c]	-	125.6[c]	-
B-2	114.3	-	114.3	-	114.0	-	114.1	-
B-3	145.0	-	145.0	-	144.0	-	144.0	-
B-4	136.1	-	136.0	-	135.9	-	135.9	-
B-5	144.1	-	144.1	-	144.8	-	144.8	-
B-6	107.1	6.38 (s)	107.2	6.36 (s)	106.9	6.33 (s)	106.9	6.33 (s)
B-7	169.3	-	169.3	-	169.7	-	169.7	-
C-1	143.7	-	143.8	-	125.7[c]	-	125.7[c]	-
C-2	129.2	-	129.2	-	112.1	-	112.1	-
C-3	159.3	-	159.3	-	145.1	-	145.1	-
C-4	160.6	-	160.6	-	136.5	-	136.5	-
C-5	149.6	-	149.6	-	146.5	-	146.5	-
C-6	108.0	7.03 (s)	108.0	6.97 (s)	106.9	6.53 (s)	106.9	6.55 (s)
C-7	163.8	-	163.8	-	168.1	-	168.1	-
D-1	124.6[b]	-	124.6[b]	-	146.0	-	146.0	-
D-2	112.1	-	112.1	-	125.1	-	125.1	-
D-3	146.9	-	146.9	-	161.9	-	161.9	-
D-4	136.5	-	136.5	-	163.5	-	163.5	-
D-5	145.4	-	145.5	-	155.6	-	155.6	-
D-6	107.7	6.72 (s)	107.8	6.71 (s)	105.8	7.03 (s)	105.8	7.02 (s)
D-7	168.1	-	168.1	-	165.0	-	165.1	-

[a] Measured in acetone-d_6+D_2O, [b,c] Assignments may be interchanged in each co

The ^{1}H NMR coupling constants of glucose H-5, 6a, and 6b of **4** (β-anomer: $J_{5,6a}$ = 1.7 Hz; $J_{5,6b}$ = 6.9 Hz) were more similar to those of strictinin with 4,6-(*S*)-HHDP ($J_{5,6a}$ = < 2 Hz; $J_{5,6b}$ = 6.3 Hz) than those of neostrictinin with 4,6-(*R*)-HHDP ($J_{5,6a}$ = 9.8 Hz; $J_{5,6b}$ = 5.6 Hz).[10] Therefore, the atropisomerism of the C-D ring linkage in **4** was suggested to be *S*. To confirm the total structure of **4,** density functional theory (DFT)

calculation of NMR chemical shifts for the (*S*)-**4** and (*R*)-**4** isomers, along with (*S*)-**4a** and (*R*)-**4a** isomers, was performed. Following a conformational search with the MMFF94 force field, the obtained conformers within an energy window of 6 kcal/mol were optimized at the B3LYP/6-31G(d,p) level in acetone using the polarizable continuum model (PCM). The lowest-energy conformers of (*S*)-**4** and (*R*)-**4** were shown in Figure 5. Conformations of the glucose moieties of (*S*)-**4** and (*R*)-**4** were very similar to those of strictinin and neostrictinin, respectively.[10] The ^{1}H and ^{13}C NMR chemical shifts of low-energy conformers with Boltzmann populations greater than 1% were calculated by DFT using the gauge-including atomic orbital (GIAO) method at the mPW1PW91/6-311+G(2d,p) level in acetone (PCM).[11] The calculated values for (*S*)-**4** agreed well with the experimental data of **4** [^{1}H NMR chemical shifts: R^2 = 0.9759 for (*S)*-**4**, 0.9386 for (*R*)-**4**, 0.8251 for (*S*)-**4a**, 0.9686 for (*R*)-**4a**; ^{13}C NMR chemical shifts: R^2 = 0.9945 for (*S)*-**4**, 0.9929 for (*R*)-**4**, 0.9889 for (*S*)-**4a**, 0.9876 for (*R*)-**4a**] (see Figs. S1 and S2 in supporting information). DP4[12] and DP4+[13] probability analyses were also performed based on calculated data, and both analyses gave a 100.0% probability for the (*S)*-**4**, supporting the validity of the structure of **4** (Fig. 2). The product **4** was tentatively named pedunculagin Ox-1. The results indicated that the atropisomerism of the biphenyl bond of the HHDP group of **1** was retained after oxidative cleavage of the

pyrogallol ring.

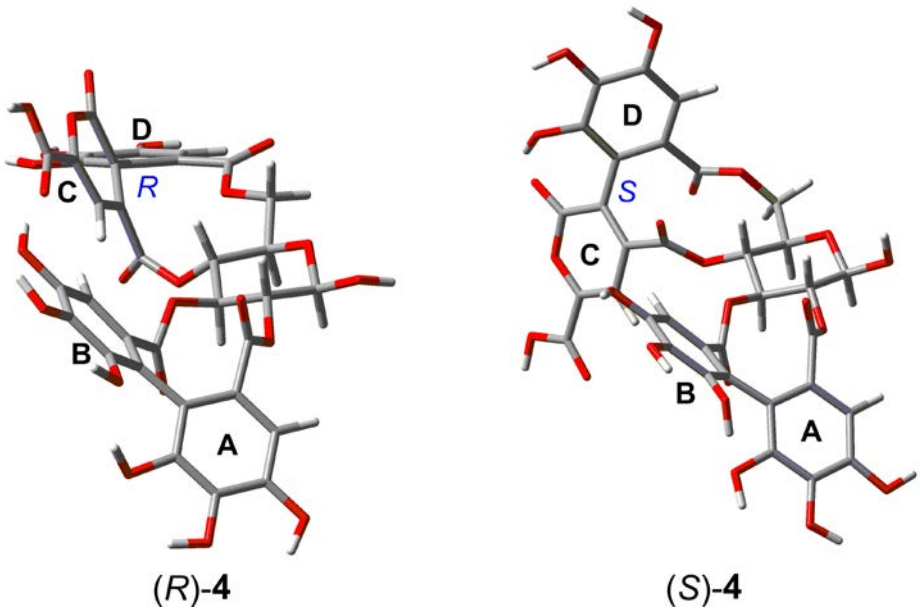

Fig. 5. Lowest-energy conformers of (*R*)-**4** and (*S*)-**4** at the B3LYP/6-31G(d,p) level in acetone (PCM).

Another oxidation product **5**, named pedunculagin Ox-2, was shown to be an isomer of **4** by high-resolution (HR)-fast atom bombardment (FAB)-MS, which exhibited a $[M+Na]^+$ peak at *m/z* 821.0444 (Calcd. for $C_{34}H_{22}O_{23}Na$ = 821.0443). Comparison of ^1H and ^{13}C NMR data (Table 1) indicated that the structural components of **5** were the same as those of **4**, and the HMBC spectrum showed that the 2*H*-2-oxo-pyran-6-

carboxylic acid unit was attached to glucose C-6. The ^{1}H NMR chemical shifts and the coupling constants of the glucose moiety of **5** were similar to those of **4**, which indicated that the absolute configuration around the C-D ring linkage in **5** was also *S*. DFT calculation of NMR chemical shifts for the (*S*)-**5**, (*R*)-**5**, (*S*)-**5a** and (*R*)-**5a** isomers was performed in a manner similar to that described for **4**. The calculated values for (*S*)-**5** agreed well with the experimental data of **5** [DP4 probability: 100.0% for (*S*)-**5**; DP4+ probability: 100.0% for (*S*)-**5**], which strongly supported the structure of **5** as shown in Figure 2.

A plausible mechanism for production of **4** and **5** from **1** (Scheme 1) involves coupled oxidation with **2**, and production of hydrogen peroxide by reduction of the oxygen molecule by **2**.[14] However, **4** and **5** were minor products, and the results of the above experiments are not sufficient to explain the decrease in the level of **1** in the *C. japonica* leaves. The initial reaction mixture obtained from **1** and **2** contained oligomeric products, which were detected at the origin on TLC and observed as a broad hump on the HPLC baseline. Oxidation of **1** in the presence of (–)-epicatechin (**3**), instead of **2**, also afforded **4** and **5** along with oligomeric products. The oligomeric products were separated by gel-permeation chromatography.[15] The ^{13}C NMR spectrum showed signals attributable to both ellagitannins and flavan-3-ols, suggesting co-oligomerization

of **1** and flavan-3-ols in the oxidation reaction (Fig. S3). Unfortunately, attempts to identify the monomeric conjugates of flavan-3-ols and ellagitannins in the mixture failed.

2.2 Separation of ellagitannin metabolites from partially matured leaves of *C. japonica*

Next, we examined whether the oxidation products **4** and **5** were produced in partially matured leaves of *C. japonica* collected in May. The aqueous acetone extract of the fresh leaves was subjected to Sephadex LH-20 column chromatography with the same solvent system as used for separation of **4** and **5**; however, **4** and **5** were not detected in the fractions. Instead, two ellagitannin metabolites **6** and **7** were isolated.

The ^{1}H and ^{13}C NMR spectra of **6** and **7** were similar to each other and showed signals arising from flavan-3-ol and ellagitannin moieties. By spectroscopic comparison, **7** was identified as camelliatannin G, which has been isolated from the same plant source before.[6c] Compound **6** was a new compound, and was shown to be an isomer of **7** by HR-electrospray ionization (ESI)-MS (*m/z* 1085.1114 $[M-H]^-$, Calcd. for $C_{27}H_{19}O_{19}$: 1085.1113). The ^{1}H and ^{13}C NMR spectra (Table 2) showed signals arising from a flavan-3-ol unit, a HHDP group, and an oxidized HHDP moiety, as well as an open-chain glucose with *C*-glycosidic nature, which were closely related to the signals observed for

7. The large coupling constant ($J_{2,3}$ = 6.9 Hz) of the C-ring H-2 showed the flavan-3-ol unit was catechin with a 2,3-*trans* configuration, and this was supported by comparison of its C-ring carbon chemical shifts (δ_C 82.2, C-2; δ_C 68.0, C-3) with those of (+)-catechin (δ_C 82.3, C-2; δ_C 68.0, C-3).[16] Connection of glucose C-1 to C-8 of the catechin unit was apparent from HMBC of the catechin A-ring C-8a (δ_C 152.1) with the C-ring H-2 (δ_H 4.84) and glucose H-1 (δ_H 4.76) (Fig. 6).

Table 2. ^{13}C (125 MHz) and ^{1}H (500 MHz) NMR data for camelliatannin I (**6**) (δ in ppm, J in Hz).

Position	^{13}C	^{1}H	Position	^{13}C	^{1}H
Glucose-1	50.6	4.76 (s)	D-Ring 1	137.9	-
2	78.7	5.63 (d, 1.0)	2	132.1	-
3	75.5	5.51 (dd, 1.0, 3.3)	3	162.7	-
4	77.3	5.09 (dd, 3.3, 8.7)	4	168.5	-
5	69.3	4.03 (m)	5	100.1	-
6a	68.4	3.70 (d, 12.3)	6	86.8	-
6b		4.70 (dd, 3.2, 12.3)	7	166.4	-
Catechin C-ring 2	82.2	4.84 (d, 6.9)	E-Ring 1	127.2 [b]	-
3	68.0	4.04 (m)	2	112.4	-
4	27.3	2.51 (dd, 7.2, 16.4)	3	146.9 [d]	-
		2.70 (dd, 5.2, 16.4)	4	137.2	-
A-ring 4a	103.0	-	5	147.9 [d]	-
5	158.6	-	6	106.4	6.46 (s)
6	90.8	5.90 (s)	7	168.5	-
7	159.2	-	F-Ring 1	125.1 [b]	-
8	104.9	-	2	116.0	-
8a	152.1	-	3	145.8 [c]	-
B-ring 1	131.7	-	4	137.0	-
2	114.1	6.81 (d, 2.1)	5	144.7 [c]	-
3	146.1	-	6	107.7	6.53 (s)
4	146.1	-	7	169.1	-
5	116.5	6.77 (d, 8.4)	G-Ring 1	125.7 [b]	-
6	120.9	6.63 (dd, 2.1, 8.4)	2	116.5	-
			3	144.8 [a]	-
			4	137.6	-
			5	145.8 [a]	-
			6	109.1	6.66 (s)
			7	170.9	-

Measured in CD_3OD. [a-d)]Assignments may be interchanged.

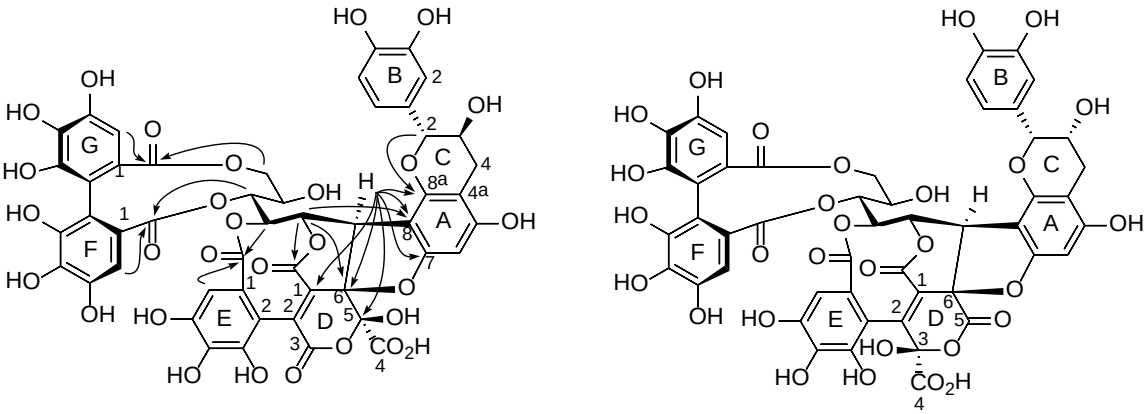

Fig. 6. Structures and important HMBC results for **6** and **7**.

A lactone ring moiety (D-ring) generated by oxidative cleavage of the aromatic ring connected to the glucose C-1 and C-2 was composed of three carboxyl groups (δ_C 162.7, C-3; δ_C 168.5, C-4; and δ_C 166.4, C-7), a double bond (δ_C 137.9, C-1 and δ_C 132.1, C-2), a hemiacetal carbon (δ_C 100.1, C-5) and an oxygenated quaternary carbon (δ_C 86.8, C-6). These were similar to that of D-ring moiety of **7**, but with a different arrangement of the carbons. HMBC of glucose H-1 to the D-ring C-1, C-6, and C-5, and of glucose H-2 to the C-6 and C-7, determined the connectivity between the glucose C-1 and D-ring C-6. Although no correlation was observed for the D-ring with C-2, -3 or -4, the structure of the D-ring was deduced from the mechanism for production from the

pyrogallol ring (Scheme S1) and the structural relationship to **7**. The chemical shift of the D-ring C-6 (δ_C 86.8) was similar to that of **7** (δ_C 86.6), which indicated an ether ring formed between the A-ring C-7 hydroxy group and D-ring C-6. In the ^{1}H NMR spectrum, glucose H-1 showed a singlet signal, which revealed that the absolute configuration of the glucose C-1 was *R* because glucose H-1 of **7** also showed a singlet signal.[6c] The absolute configuration of the oxygenated quaternary carbon (C-6) at the D-ring was also assigned as *R*, since the (6*S*)-form had a highly strained structure in molecular modeling. The negative Cotton effect at 257 nm and positive Cotton effect at 236 nm indicated the HHDP groups at the glucose 4 and 6 positions were in the *S* configuration. However, the stereochemistry at the hemiacetal carbon C-5 of the D-ring could not be determined from the spectroscopic data. Therefore, DFT calculations of ^{13}C NMR chemical shifts of low-energy conformers for (5*R*)-**6** and (5*S*)-**6** with Boltzmann populations greater than 1% were performed. Comparison of experimental data and Boltzmann-weighted calculated data showed that the calculated data for both (5*R*)-**6** and (5*S*)-**6** agreed with the experimental data, and the difference between (5*R*)-**6** and (5*S*)-**6** was very small (R^2 = 0.9963 for 5*R*, and R^2 = 0.9962 for 5*S*) (Fig. S6, S7). However, DP4 probability analysis afforded 61.0% probability, and DP4+ analysis gave 72.2% probability for the (5*R*)-structure from calculated ^{13}C NMR chemical shifts. We

also examined the differences between experimental and calculated ^{13}C NMR chemical shifts in the D-ring moiety, which will be affected by changes in the absolute configuration at C-5. The calculated ^{13}C NMR chemical shifts of D-ring C-3, C-5, and C-6 in (5*R*)-**6** showed smaller errors than (5*S*)-**6**. This was a strong indication that the absolute configuration of the D-ring C-5 was *R* (Fig. 7). From these results, the structure of **6** was proposed (Fig. 6), and this compound was named camelliatannin I.

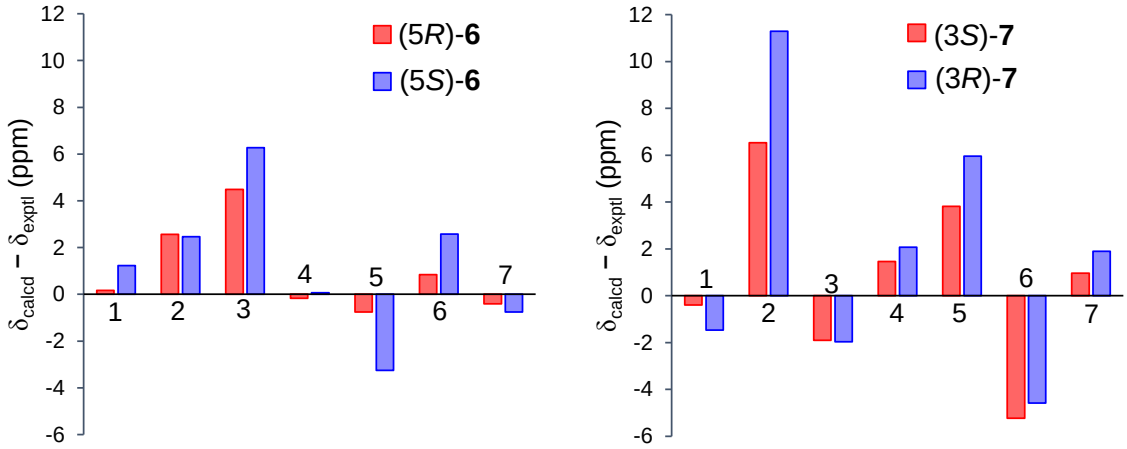

Fig. 7. Differences between experimental and calculated ^{13}C NMR chemical shifts of the D-ring moiety in **6** and **7**. Δδ (ppm) = $\delta_{calcd.} - \delta_{exptl}$. Calculations of NMR chemical shifts were performed at the mPW1PW91/6-311+G(2d,p) level in MeOH (**6**) or acetone (**7**) (PCM) and linearly corrected for the experimental data.

For known compound **7**, the absolute configuration of the hemiacetal carbon C-3 at the D-ring has not been assigned. Therefore, we investigated its absolute configuration by DFT calculation of ^{13}C NMR chemical shifts in a similar manner (Fig. S8 – S11). There was greater agreement between the experimental ^{13}C NMR chemical shifts and the calculated data for (3*S*)-**7** than that for (3*R*)-**7** [R^2 = 0.9954 for (3*S*)-**7**; R^2 = 0.9930 for (3*R*)-**7**]. In addition, both DP4 and DP4+ analyses showed that the (3*S*) structure had 100.0% probability. We also examined the difference between experimental and calculated ^{13}C NMR chemical shifts for the D-ring moiety. The calculated ^{13}C NMR chemical shifts for D-ring C-2 and C-5 in (3*S*)-**7** apparently showed smaller errors than those of (3*R*)-**7** (Fig. 7). These data suggested the absolute configuration of C-3 at the D-ring was *S* (Fig. 6). The plausible mechanism for production of compounds **6** and **7** is as follows: first an intramolecular C-glycosidic linkage between anomeric carbon and the HHDP group is formed in the molecule of **1**. Subsequent conjugation of flavan-3-ol at the glucose C-1 and oxidative cleavage of the pyrogallol ring accompanied by reaction with an A-ring phenolic hydroxy group generates **6** and **7** (Scheme S1).

3. Conclusions

We found seasonal changes occurred in the levels of pedunculagin (**1**) and catechin (**2**) in the leaves of *C. japonica,* and we assume this is caused by oxidative degradation of **1** by enzymes. In vitro model experiments showed that **1** is oxidized by coupled oxidation with catechol-type catechin (**2** or **3**), and the structures of oxidation products **4** and **5** were established by spectroscopic and computational methods. We did not detect these products in mature leaves. However, two ellagitannin metabolites (**6** and **7**) were isolated from a fraction, which was eluted with a solvent similar to that used for **4** and **5**. Their structures suggest coupling of the production of **1** with flavan-3-ols, and subsequent oxidation of the leaves. The decrease in the level of **1** cannot be explained by simple oxidative cleavage of the pyrogallol rings, and coupling with the electron-rich A-ring C-8 and C-6 of catechins and/or procyanidins may occur.[6] However, although we found an oligomeric mixture (Fig. S3), we did not identify any catechin-ellagitannin conjugates in our oxidation experiments of **1**. Interestingly, the ^{13}C NMR spectrum of oligomeric polyphenols isolated by gel-permeation chromatography from leaves collected in April indicated the oligomers in these leaves are procyanidins (Fig. S3). However, the spectrum of oligomers obtained from leaves collected in August (Fig. S12) showed signals for ellagitannin moieties and flavan-3-ol moieties, which were

similar to those observed in the spectrum of oligomeric products obtained from **1** and **3**. Further investigations to understand the catechin-ellagitannin co-oligomerization are now underway.

4. Experimental

4.1. General experimental procedures

IR and UV spectra were obtained with Jasco FT/IR-410 and Jasco V-560 UV/Vis spectrophotometers (Jasco Co., Tokyo, Japan). Optical rotations were measured on a Jasco P-1020 digital polarimeter (Jasco Co.). Elemental analysis was conducted with a Perkin Elmer 2400 II analyzer (PerkinElmer Inc., Waltham, MA). ^{1}H NMR, ^{13}C NMR, ^{1}H-^{1}H COSY, HSQC, and HMBC spectra were measured on a Varian Unity plus 500 spectrometer operating at 500 and 125 MHz for the ^{1}H and for ^{13}C spectra, respectively (Varian, Palo Alto, CA), or a JEOL JNM-AL 400 spectrometer operating at 400 and 100 MHz for the ^{1}H and ^{13}C NMR, respectively (JEOL Ltd., Tokyo, Japan). Coupling constants (*J*) are expressed in Hz, and chemical shifts (δ) are in ppm. ESI-MS were obtained using a JEOL JMS-T100TD spectrometer (JEOL Ltd.). High-resolution FAB-MS were recorded on a JMS 700N spectrometer (JEOL Ltd.), using *m*-nitrobenzyl alcohol or glycerol as the matrix. Column chromatography was conducted using Diaion

HP20SS and MCI gel CHP-20P (Mitsubishi Chemical Co., Tokyo, Japan), Sephadex LH-20 (25–100 μm, GE Healthcare UK Ltd., Little Chalfont, UK), Chromatorex ODS (Fuji Silysia Chemical Ltd., Kasugai, Japan), and silica gel 60N (100–210 μm, Kanto Chemical Co., Tokyo, Japan) columns. TLC was performed on precoated Kieselgel 60 F_{254} plates (0.2 mm thick, Merck, Germany) with toluene/ethyl formate/formic acid (1/7/1, v/v/v). Cellulose F plates (0.1 mm thick, Merck, Darmstadt, Germany) with 2% aqueous acetic acid was also used for detection of ellagitannins. Spots were detected under ultraviolet illumination after spraying with 2% ethanolic $FeCl_3$ or 5% aqueous H_2SO_4 followed by heating. Analytical HPLC was performed on a Cosmosil 5C_{18}-ARII (Nacalai Tesque, Kyoto, Japan) column (250 × 4.6 mm i.d.) with gradient elution of CH_3CN in 50 mM H_3PO_4 from 4 to 30% (39 min) and from 30 to 75% (15 min). The mobile phase flow rate was 0.8 mL/min, the column temperature was 35 °C, and the detector was a Jasco photodiode array detector (MD-2010).

4.2. Plant material

Leaves of *C. japonica* L. were collected at the Medical Plant Garden of the Graduate School of Biomedical Sciences, Nagasaki University, and identified by Dr. Koji Yamada. A voucher specimen was deposited in the Medical Plant Garden, Nagasaki

University.

4.3. Preparation of pedunculagin (1)

Fresh young leaves of *C japonica* (1.0 kg) collected in April were homogenized in Waring blender with 70% acetone (4 L). After filtration, the filtrate was concentrated and resulting precipitate, which mainly contained chlorophyll, was removed by filtration. The filtrate was applied to a Sephadex LH-20 column (35 cm × 10 cm i.d.). A stepwise elution with 0–100% MeOH in H_2O (each step increasing MeOH volume fraction by 20%, the volume of each step was 1 L), and washing with 60% aqueous acetone (3 L), gave 12 fractions. Fraction 11 (11.1 g), which contained **1** as the major component, was selected for further fractionation on a Chromatorex ODS column chromatography (25 cm × 4 cm i.d., stepwise elution with 0–50% MeOH in H_2O). This gave **1** (7.98 g) as an amorphous powder.

4.4. Oxidation of pedunculagin (1)

Japanese pear fruit (100 g), purchased at local market, was homogenized with 100 mL of H_2O and filtered through four layers of gauze. The filtrate (100 mL) was mixed with 100 mL of an aqueous solution of **1** (1.08 g, 1.38 mmol) and **2** (0.20 g, 0.69 mmol)

and vigorously stirred at room temperature for 2 h. Then, the solution was mixed with acetone (900 mL) and filtered. The filtrate was concentrated to 100 mL and fractionated on a Sephadex LH 20 column (25 cm × 3 cm i.d.). Elution with 40–100% MeOH (stepwise elution, each step 200 mL and the MeOH volume fraction increased by 10%), and washing with 60% acetone, gave a fraction (331 mg) containing **4** and **5**. The recoveries of **1** and **2** were 388 mg and 104 mg, respectively. This fraction was subjected to MCI-gel CHP20P column chromatography (20 cm × 2 cm i.d., 0–100% MeOH stepwise elution) to give three fractions. Fraction 1 (104 mg) was purified on a Chromatorex ODS column (20 cm × 2 cm i.d., 0–20% MeOH stepwise elution) to obtain **4** (47 mg). Fraction 2 (84 mg) was purified by Chromatorex ODS column chromatography (20 cm × 2 cm i.d., 0–20% MeOH stepwise elution) to obtain **5** (7 mg).

*4.4.1. Pedunculagin Ox-1 (**4**)*

Brown amorphous powder. $[\alpha]_D^{30}$ +16.6 (*c* 0.20, MeOH). IR (dry film) cm^{-1}: 3418, 1745, 1729, 1716, 1616, 1358, 1189. UV λ_{max} (MeOH) nm (log ε): 341 (3.42), 254 (4.04), 216 (4.36), 204 (4.35). FAB-MS *m/z*: 799 $[M+H]^+$. Anal. Calcd. for $C_{34}H_{22}O_{23}3.5H_2O$: C, 47.04; H, 3.39. Found: C, 47.11; H, 3.18. ^1H and ^{13}C NMR data: see Table 1.

*4.4.2. Pedunculagin Ox-2 (**5**)*

Brown amorphous powder. $[\alpha]_D$ +1.15 (*c* 0.20, MeOH). IR (dry film) cm^{-1}: 3390, 1739,

1730, 1714, 1614, 1359, 1182. UV λ_{max} (MeOH) nm (log ε): 325 (3.87), 255 (4.33), 215 (4.60). FAB-MS *m/z*: 799 $[M+H]^+$. HR-FAB-MS *m/z*: 821.0444 (Calcd. for $C_{34}H_{22}O_{23}Na$: 821.0443). ^1H and ^{13}C NMR data: see Table 1.

4.5. Oligomeric oxidation products from 1 and 3

A mixture of **1** (1.08 g) and (–)-epicatechin (**3**) (0.20 g) was oxidized for 2 h in a manner similar to that described in Section 4.4 The product was fractionated by Sephadex LH 20 column chromatography (20 cm × 3 cm i.d.). After a 0–100% MeOH stepwise elution, and washing with 60% aqueous acetone, seven fractions were obtained. Fraction 5 (328 mg), which contained oligomeric products and ellagitannins, was fractionated further by gel-permeation chromatography using a Sephadex LH 20 column (50 cm × 4 cm i.d.) and elution with acetone-7 M urea (3:2, v/v, adjusted to pH 2 with HCl). Urea was removed by Diaion HP20SS column chromatography to give a mixture of compounds containing **4** and **5** (167 mg) and an oligomer fraction (56 mg).

*4.5.1. Oligomeric polyphenol fraction from **1** and **3***

Brown amorphous powder. IR (dry film) cm^{-1}: 3390, 1730, 1615, 1517, 1446, 1325, 1230. UV λ_{max} (MeOH) nm: 269 (sh), 204. Elemental analysis: Found: C, 49.61; H, 4.30.

4.6. Isolation of 6 and 7 from the leaves

Fresh *C. japonica* leaves (1.0 kg) collected at the end of May 2015 were extracted with 70% acetone (4 L, three times). The combined extract was concentrated until the acetone was completely evaporated. After removal of any insoluble material by filtration, the filtrate was subjected to column chromatography over Sephadex LH 20 (35 cm × 10 cm i.d.). After a stepwise elution with 0–100% MeOH (each step 500 mL and the MeOH volume fraction increased by 20%), and washing with 70% acetone, 12 fractions were obtained. Fraction 7 (1.44 g) was fractionated further by MCI-gel CHP20P column chromatography (20 cm × 4 cm i.d., 0–100% MeOH, 10% stepwise elution) to give two fractions. Fraction 7-1 (135 mg) was purified on a Chromatorex ODS column (20 cm × 2 cm i.d., 0–100% MeOH) to obtain camelliatannin I (**6**) (87 mg) and camelliatannin G (**7**) (42 mg).

*4.6.1. Camelliatannin I (**6**)*

Brown amorphous powder. $[\alpha]_D^{30}$ −100.9 (*c* 0.10, MeOH). IR (dry film) cm^{-1}: 3432, 1737, 1621, 1515, 1450, 1321, 1224, 1097, 1047. UV λ_{max} (MeOH) nm (log ε): 279 (sh, 4.57), 234 (sh, 4.99), 212 (5.19). ESI-MS *m/z:* 1085 $[M-H]^-$. HR-ESI-MS *m/z*: 1085.1114 $[M-H]^-$ (Calcd. for $C_{27}H_{19}O_{19}$: 1085.1113). ECD (MeOH) λ_{max} ($\Delta\varepsilon$); 311 (–3.39), 281 (+3.06), 257 (–14.4), 236 (+16.8). ^1H and ^{13}C NMR (CD_3OD): see Table 2.

*4.6.2. Camelliatannin G (**7**)*

Brown amorphous powder. ^{1}H NMR (CD_3OD): δ 2.59 (1H, dd, *J*=4.9, 16.4 Hz H-4), 2.84 (1H, dd, *J*=4.5, 16.4 Hz H-4), 3.58 (1H, d, *J*=12.3 Hz, glc-H-6), 4.04 (1H, dd, *J*=2.7, 8.4 Hz glc-H-5), 4.20 (1H, m, H-3), 4.67 (1H, dd, *J*=2.7, 12.3 Hz glc-H-6), 5.06 (1H, br, H-2), 5.10 (1H, dd, *J*=4.1, 8.4 Hz, glc-H-4), 5.52 (1H, br d, *J*=4.1 Hz, glc-H-3), 5.73 (1H, br, glc-H-2), 5.91 (1H, s, H-6), 6.44 (1H, s, E-ring H-6), 6.48 (1H, s, G-ring H-6), 6.69 (1H, s, F-ring H-6), 6.72 (1H, dd, *J*=1.7, 8.1 Hz, B-ring H-6), 6.76 (1H, d, *J*=8.1 Hz, B-ring H-5), 7.00 (1H, d, *J*=1.7 Hz, B-ring H-2).

4.7. Isolation of oligomeric polyphenols from the leaves

Fresh *C. japonica* leaves (1.0 kg) collected in August were extracted with 60% acetone (5 L). The extract was concentrated and the resulting precipitate was removed by filtration. The aqueous solution was subjected to column chromatography over Sephadex LH-20 (33 cm × 5 cm i.d.). The column was eluted with 0–100% MeOH in H_2O in a stepwise elution with each step using 300 mL and the MeOH volume fraction increased by 20%, and then 60% acetone, to give two fractions. Fraction 2, which mainly contained polyphenols, was fractionated further by Diaion HP20SS column chromatography (21 cm × 5 cm i.d. using a stepwise elution with 0–100% MeOH in H_2O.

Fractions 2-1 (31.92 g), which contained polyphenols, and 2-2 (12.13 g), which contained saponins and flavonol glycosides, were retained. Some of fraction 2-1 (10.0 g) was subjected to gel-permeation chromatography on Sephadex LH-20 (50 cm × 4 cm i.d.) and eluted with acetone-7 M urea (3:2, v/v, adjusted to pH 2 with concentrated HCl) to give three fractions: Fraction 2-1-1 contained high MW polyphenols. Urea was removed from fractions 2-1-2 and 2-1-3 using Diaion HP20SS. Fraction 2-1-2 (5.04 g) was a mixture of high and low MW polyphenols, and Fr. 2-1-3 was a mixture of low MW polyphenols. Fr. 2-1-1 was concentrated to remove acetone, and the aqueous solution was applied to a Diaion HP 20 SS column (20 cm × 4 cm i.d.). After washing with water to remove urea and HCl, the column was eluted with 10–100% MeOH. Two fractions, 2-1-1-1 (780 mg) and 2-1-1-2 (1.20 g), were collected and fraction 2-1-1-1 was further purified on a Chromatorex ODS column (20 cm × 3 cm i.d.). This was eluted with 0–100% MeOH to give a fraction (530 mg) containing oligomeric polyphenols. Oligomeric polyphenols from leaves collected in April were isolated using a similar procedure.

4.6.1. Oligomeric polyphenol fraction from leaves collected in August.

Brown amorphous powder. IR (dry film) cm^{-1}: 3417, 1731, 1615, 1519, 1454, 1286, 1204. UV λ_{max} (MeOH) nm : 274 (sh), 204. Elemental analysis: Found: C, 52.09; H, 4.76.

4.6.1. Oligomeric polyphenol fraction from leaves collected in April.

Brown amorphous powder. IR (dry film) cm^{-1}: 3392, 1615, 1521, 1445, 1362, 1285, 1246, 1207. UV λ_{max} (MeOH) nm : 280, 204. Elemental analysis: Found: C, 53.83; H, 4.45.

4.8. DFT calculations of NMR chemical shifts.

A conformational search was performed using the Monte Carlo method and the MMFF94 force field with Spartan 14 (Wavefunction, Irvine, CA). The obtained low-energy conformers within 6 kcal/mol were optimized at the B3LYP-SCRF/6-31G(d,p) level in MeOH (**6**) or acetone (**4**, **5**, and **7**) (PCM). The vibrational frequencies were also calculated at the same level to confirm their stability, and no imaginary frequencies were found. The ^{1}H and ^{13}C NMR chemical shifts of the low-energy conformers with Boltzmann populations greater than 1% were calculated using the gauge-including atomic orbital (GIAO) method at the mPW1PW91-SCRF/6-311+G(2d,p) level in MeOH (**6**) or acetone (**4**, **5**, and **7**) (PCM).[11] Calculated NMR chemical shifts were linearly corrected for the experimental data. All DFT calculations were performed using Gaussian 09.[17] GaussView was used to draw the three-dimensional molecular structures.[18]

Acknowledgments

This work was supported by the Japan Society for the Promotion of Science KAKENHI (Grant Nos. 26460125 and 16K07741). The authors are grateful to Mr. K. Inada, Mr. N. Tsuda, and Dr. K. Chifuku (Center for Industry, University and Government Cooperation, Nagasaki University) for NMR, MS, and elemental analysis measurements. The computational analysis was partly carried out using the computer facilities at the Research Institute for Information Technology, Kyushu University.

References

1. (a) Hagerman, A. E., **2012**, In *Recent Advances in Polyphenol Research*; Cheynier V., Sarni-Manchado, P., Quideau S., Ed.; Wiley, 2012; Vol. 3, pp71-95; (b) Robbins, C. T.; Hanley, T. A.; Hagerman, A. E.; Hjeljord, O.; Baker, D. L.; Schwartz, C. C.; Mautz, W. W. *Ecology* **1987**, *68*, 98-107.

2. (a) Zucker, W. V. *The American Naturalist* **1983**, *121*, 335-365; (b) Barbehenn, R. V.; Constabel, C. P. *Phytochemistry* **2011**, *72*, 1551–1565.

3. (a) Feeny, P. P.; Bostock, H. *Phytochemistry* **1968**, *7*, 871–880; Feeny, P. P., *Ecology* **1970**, *51*, 565–581.

4. Tanaka, T.; Takahashi, R.; Kouno, I.; Nonaka, G. *J. Chem. Soc. Perkin Trans. 1*, **1994**, 3013-3022.

5. (a) Cooper, S. M.; Owen-Smith, N.; Bryant, J. P. 1988. *Oecologia*, **1988**, *75*, 336-342; (b) Hagerman, A. E. *J. Chem. Ecol*. **1988**, *14*, 453-461; (c) Salminen, J. P.; Roslin, T.; Karonen, M.; Sinkkonen, J.; Pihlaja, K.; Pulkkinen, P. *J. Chem. Ecol*. **2004**, *30*, 1693-1711; (d) Riipi, M.; Ossipov, V.; Lempa, K.; Haukioja, E.; Koricheva, J.; Ossipova, S.; Pihlaja, K. *Oecologia* **2002**, *130*, 380-390; (e) Dement, W. A.; Mooney, H. A. *Oecologia* **1974**, *15*, 65-76; (f) Hatano, T.; Kira, R.; Yoshizakia, M.; Okuda, T. *Phytochemistry* **1986**, *25*, 2787–2789.

6. (a) Yoshida, T.; Chou, T.; Maruyama, Y.; Okuda, T. *Chem. Pharm. Bull*., **1990**, *38*, 2681-2686; (b) Hatano, T.; Shida, S.; Han, L.; Okuda, T. *Chem. Pharm. Bull.* **1991**, *39*, 876-880; (c) Han, L.; Hatano, T.; Yoshida, T.; Okuda, T. *Chem. Pharm. Bull*. **1994**, *42*, 1399-1409; (d) Hatano, T.; Han, L.; Taniguchi, S.; Shingu, T.; Okuda, T.; Yoshida, T. *Chem. Pharm. Bull*. **1995**, *43*, 1629-1633; (e) Hatano, T.; Han, L., Taniguchi, S., Okuda, T.; Kiso, Y.; Tanaka, T.; Yoshida, T. *Chem. Pharm. Bull*., **1995**, *43*, 2033-2035.

7. (a) Haslam, E. *Phytochemistry* **2003**, *64*, 61–73; (b) Tanaka, T.; Matsuo, Y.; Kouno, I. *Int. J. Mol. Sci.* **2010**, *11*, 14–40; (c) Tanaka, T.; Mine, C.; Inoue, K.; Matsuda, M.; Kouno, I. *J. Agric. Food Chem.*, **2002**, *50*, 2142-2148.

8. Guyot, S.; Vercauteren, J.; Cheynier, V. *Phytochemistry*, **1996**, *42*, 1279—1288.

9. Robertson, A. *Phytochemistry*, **1983**, *22*, 889-896.

10. Era, M.; Matsuo, Y.; Shii, T.; Saito, Y.; Tanaka, T.; Jiang, Z.-H. *J. Nat. Prod*. **2015**, *78*, 2104-2109.

11. (a) Lodewyk, M. W.; Siebert, M. R.; Tantillo, D. J. *Chem. Rev.* **2012**, *112*, 1839–1862; (b) Willoughby, P. H.; Jansma, M. J.; Hoye, T. R. *Nat. Protoc*. **2014**, *9*, 643–660; (c) Grimblat, N.; Sarotti, A. M. *Chem. Eur. J*. **2016**, *22*, 12246–12261.

12. Smith, S. G.; Goodman, J. M. *J. Am. Chem. Soc*. **2010**, *132*, 12946-12959.

13. Grimblat, N.; Zanardi, M. M.; Sarotti, A. M. *J. Org. Chem*. **2015**, *80*, 12526-12534.

14. (a) Subramanian, N.; Venkatesh, P.; Ganguli, S.; Sinkar, V. P. *J. Agric. Food Chem*., **1999**, *47*, 2571-2578; (b) Nakayama, T.; Ichiba M.; Kuwabara, M.; Kajiya, K.; Kumazawa, S. *Food Sci. Technol. Res*., **2002**, *8*, 261-267; (c) Akagawa, M.; Shigemitsu, T.; Suyama, K. *Biosci. Biotechnol. Biochem*. **2003**, *67*, 2632-2640.

15. Yanagida, A.; Shoji, T.; Shibusawa, Y. *J. Biochem. Biophys. Methods*, **2003**, *56*, 311–322.

16. Nonaka, G.; Ezaki, E.; Hayashi, K.; Nishioka, I. *Phytochemistry* **1983**, *22*, 1659-1661.

17. Frisch, M. J.; Trucks, G. W.; Schlegel, H. B.; Scuseria, G. E.; Robb, M. A.; Cheeseman, J. R.; Scalmani, G.; Barone, V.; Mennucci, B.; Petersson, G. A.; Nakatsuji, H.; Caricato, M.; Li, X.; Hratchian, H. P.; Izmaylov, A. F.; Bloino, J.; Zheng, G.; Sonnenberg, J. L.; Hada, M.; Ehara, M.; Toyota, K.; Fukuda, R.; Hasegawa, J.; Ishida, M.; Nakajima, T.; Honda, Y.; Kitao, O.; Nakai, H.; Vreven, T.; Montgomery, J. A., Jr.; Peralta, J. E.; Ogliaro, F.; Bearpark, M.; Heyd, J. J.; Brothers, E.; Kudin, K. N.; Staroverov, V. N.; Kobayashi, R.; Normand, J.; Raghavachari, K.; Rendell, A.; Burant, J. C.; Iyengar, S. S.; Tomasi, J.; Cossi, M.; Rega, N.; Millam, M. J.; Klene, M.; Knox, J. E.; Cross, J. B.; Bakken, V.; Adamo, C.; Jaramillo, J.; Gomperts, R.;

Stratmann, R. E.; Yazyev, O.; Austin, A. J.; Cammi, R.; Pomelli, C.; Ochterski, J. W.; Martin, R. L.; Morokuma, K.; Zakrzewski, V. G.; Voth, G. A.; Salvador, P.; Dannenberg, J. J.; Dapprich, S.; Daniels, A. D.; Farkas, O.; Foresman, J. B.; Ortiz, J. V.; Cioslowski, J.; Fox, D. J. Gaussian 09, Revision D.01; Gaussian, Inc.: Wallingford, CT, 2013.

18. Dennington, R.; Keith, T.; Millam, J. GaussView, Version 5.0.9; Semichem Inc.: Shawnee Mission, KS, 2009.

Legends

Fig. 1. HPLC profiles of 60% ethanol extracts of the leaves of *C. japonica*.

Compound labels are: **1**, α- and β-anomers of pedunculagin; **2**, catechin; **3**, epicatechin; and p, procyanidins

Fig. 2. Structures of major polyphenols found in *C. japonica* leaves.

Fig. 3. Decrease in the level of **1** on treatment with polyphenol oxidase

Open circle: **1** + polyphenol oxidase, solid circle: **1** + **2** + polyphenol oxidase

Fig. 4. Selected HMBC results for **4** and **5**.

Fig. 5. Lowest-energy conformers of (*R*)-**4** and (*S*)-**4** at the B3LYP/6-31G(d,p) level in acetone (PCM).

Fig. 6. Structures and important HMBC results for **6** and **7**.

Fig. 7. Differences between experimental and calculated ^{13}C NMR chemical shifts of the D-ring moiety in **6** and **7**. $\Delta\delta$ (ppm) = $\delta_{calcd.} - \delta_{exptl}$. Calculations of NMR chemical shifts were performed at the mPW1PW91/6-311+G(2d,p) level in MeOH (**6**) or acetone (**7**) (PCM) and linearly corrected for the experimental data.

Scheme 1 Plausible oxidation mechanism.